

Automatic Segmentation of Brain Tissues for Newborn MRI in Longitudinal Study

F. Shi¹, Y. Fan¹, S. Tang¹, K. Cleary², M. Styner², J. Gilmore², W. Lin¹, and D. Shen¹

¹Department of Radiology and BRIC, University of North Carolina, Chapel Hill, NC, United States, ²Department of Psychiatry, University of North Carolina, Chapel Hill, NC, United States

Introduction: Brain structure and function develop rapidly in first years of life. This rapid brain developmental process can be tracked *in vivo* with the state-of-art magnetic resonance imaging (MRI) technique. For quantitatively measuring global and local brain development in newborns, a crucial step is to segment the brain tissues into gray matter (GM), white matter (WM), and cerebrospinal fluid (CSF). However, tissue segmentation of newborn brains is challenging due to low signal contrast and poor spatial resolution. As a result, the intensity-based segmentation approaches often fail in newborn brain images. To overcome this problem, current newborn image segmentation is often guided by some prior knowledge of tissue spatial distribution derived from other individuals (i.e., a population atlas built from pre-segmented individual images). However, the performance of this population atlas-based segmentation method is still limited by several inherent drawbacks. *First*, the atlas created from a population is generally very fuzzy and cannot provide detailed distribution information for cortex. *Second*, the atlas is often affine-aligned to the subject, and thus unable to provide precise tissue distribution information for the corresponding structures. In a longitudinal study, subjects are scanned at multiple times. Since the human cortical convolution pattern is generated during gestation and remains very similar throughout the entire life span (Fig. 1), and also image segmentation is not difficult at a later age even at one-year-old, the probability maps of brain tissues obtained from images acquired at a later age can be used as subject-specific atlases to guide the segmentation of the newborn brain as we did in [1]. In this abstract, we developed a dedicated longitudinal newborn MRI segmentation framework, and further validated it with manual segmentations.

Methods: A total of 8 subjects participated in this study. MR images were acquired using a 3T Siemens scanner from each subject at three time points, e.g., postnatal age of several weeks, one year and two years, respectively. For T1 images, 160 sagittal slices were obtained with parameters: TR=1900ms, TE=4.38ms, Flip Angle=7, and resolution=1x1x1 mm³. For T2 images, 70 transverse slices were acquired with parameters: TR=7380ms, TE=119ms, Flip Angle=150, and resolution=1.25x1.25x1.95 mm³. T2 images were aligned to T1 images with rigid transform and resampled to 1x1x1 mm³. All images were skull-stripped and cerebellum-removed. The proposed segmentation framework consists of the following two components.

Subject-specific Atlas Generation: The one- or two-year-old images of each subject were segmented with a fuzzy clustering approach after bias correction [2]. Each brain voxel was assigned with three memberships representing the probabilities of this voxel belonging to GM, WM and CSF, respectively. The resulting probability maps were then used as subject-specific atlases with detailed tissue distribution information (especially in cortex). **Atlas Propagation and Segmentation:** Since brain structures change rapidly with early brain development, the subject-specific atlas obtained from the later time images should be warped to the newborn image space non-rigidly. However, it is not easy for performing direct registration between newborn and later time images due to significant difference of intensity distribution between them. Thus, a hierarchical iterative registration and segmentation strategy was adopted here. At first, the subject-specific atlas was aligned to the newborn images with affine transform, and used to guide

the tissue segmentation. In newborn image segmentation, a mixture of Gaussians model was used to model the non-Gaussian distribution of each brain tissue. Also, bias field was estimated to remove intensity inhomogeneity in the brain images. Afterwards, GM, WM and CSF were segmented from newborn images based on the warped subject-specific probability maps according to the Bayes rule [3]. Note that T1 and T2 images were integrated in our method for tissue segmentation, thus taking advantages of both modalities: high resolution in T1 images and relatively better tissue contrast in T2 images. Based on the segmentation results, the non-rigid registration between the atlas and the newborn images was refined by HAMMER [4], which was used to further bring the atlas closer to the newborn images for guiding better tissue segmentation. These two steps of registration and segmentation were repeated until convergence. It is worth noting that, the registration was performed hierarchically, i.e., allowing only global registration in the initial stage and gradually local registration in the later stage as segmentation becomes accurate. Similarly, when performing atlas-based tissue segmentation, the atlas was blurred more in the initial stage to account for the registration errors, and then blurred less in the later stage for providing more specific information for guiding segmentation. By using this whole procedure, the newborn images can be segmented.

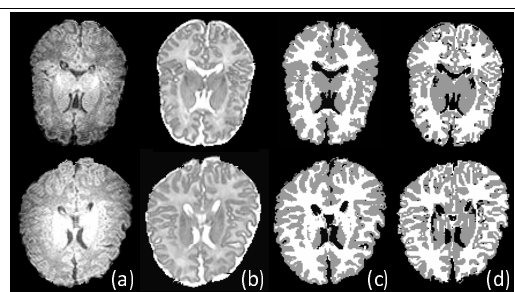


Fig. 2. Original T1 and T2 MR images (a-b), and their automatic (c) and manual (d) segmentations. Results on two subjects are shown.

Results: The segmentation results are shown in Fig. 2c. It is evident that the fine structures of the cortex were well segmented. For quantitative validation of our proposed tissue segmentation method, two expert raters manually segmented 8 T2 images (because of their T2 relatively high tissue contrast compared to T1 images) in 2 sagittal slices, 3 coronal slices, and 3 transverse slices (Fig. 2d) by using a prior initialization of the segmentation and the InsightSNAP [5]. Note that the central brain region was blocked from manual segmentation due to its low tissue contrast (Fig. 2d). Visually, automatic segmentations are close to manual segmentations. For quantitative comparison, the Dice similarity coefficient (DSC) was employed to measure the overlap rate between the two segmentation results (Fig. 3). The DSC in GM was 0.77 ± 0.02 between the proposed method and rater 1, 0.76 ± 0.02 with rater 2, and the inter-rater DSC was 0.89 ± 0.02 (which is rather high and may be due to the same initialization for the manual editing). In WM, DSC 0.80 ± 0.03 was achieved between the proposed method and rater 1, 0.77 ± 0.03 with rater 2, and the inter-rater DSC was 0.86 ± 0.02 . Volume error between two segmentations was also calculated, i.e., 0.023 with rater 1 and 0.021 with rater 2, suggesting relatively high accuracy achieved by the proposed method.

Conclusion: A longitudinal newborn MRI segmentation framework is proposed. Our segmentation framework takes advantage of longitudinal information available from each subject, through the utilization of the images obtained at a later age as subject-specific atlases to guide the newborn image segmentation. A hierarchical iterative registration and segmentation procedure is proposed to ensure the better registration of two time images and thus bring the atlases close to the newborn images for guiding better tissue segmentation. Our segmentation results were validated qualitatively by visual inspection and quantitatively by comparison with manual segmentations, both indicating that accurate segmentation results are achieved by the proposed method.

References: [1] F. Shi et al., SPIE Med. Imaging, 2009. [2] D. Pham, J. Prince, IEEE TMI, 18, 1999. [3] J. Ashburner, K. J. Friston, Neuroimage, 26, 839-851, 2005. [4] D. Shen, C. Davatzikos, IEEE TMI, 21, 2002. [5] P. Yushkevich, et al., NeuroImage 31(3), 1116-28, 2006.

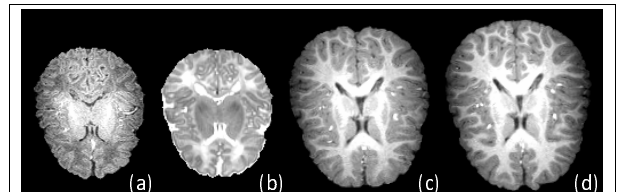


Fig. 1. Similar cortical patterns in the same subject at age of several weeks (a), one year (c), and two years (d). Here, (a), (c), and (d) are T1 images, and (b) is T2 image.

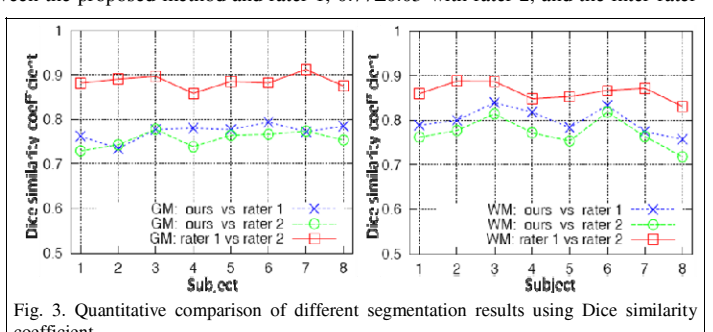


Fig. 3. Quantitative comparison of different segmentation results using Dice similarity coefficient.